1. Particle Size and Images

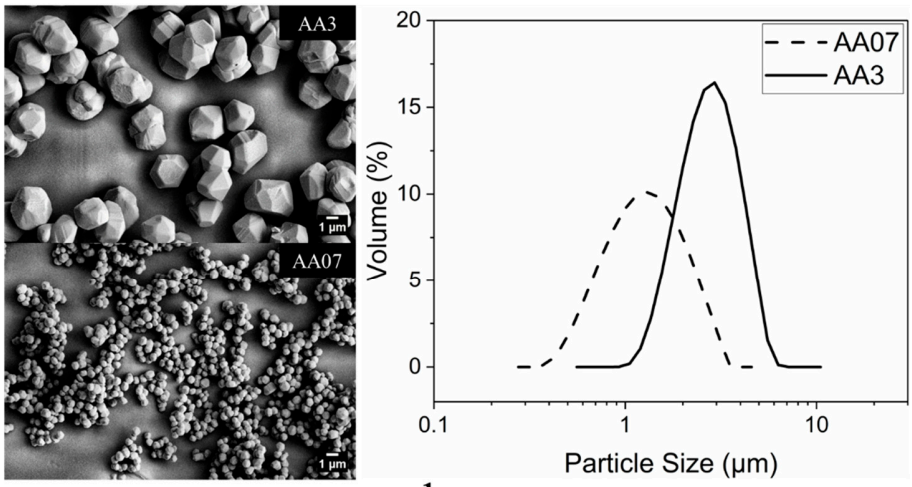

Figure S1. The powders, AA3 and AA07, were used with this study's suspensions. (a) Particle morphology, which is visualized by the use of a field emission scanning electron microscope (FESEM) (Zeiss, Oberkochen, German), and (b) particle size distribution, which is measured using a dynamic light scattering method using Mastersizer 3000 (Malvern Panalytical Ltd., Malvern, UK).

2. Resin Properties

Table S1. Acrylate based resins. The materials were a mixture of an oligomer as a backbone of the resins, and a monomer. The monomer is used to lower the viscosity of the oligomer. The cure depth was measured using an energy dose of 91.4 mJ/cm^2. The test reflects five trials with a standard deviation error. The viscosity was measured at a shear rate of 1.0 sec^{-1} and 25.0 °C. The refractive index was measured using Abbe Refractometer C10 (Vee Gee Scientific, LLC., Vernon Hills, USA) at 589 nm.

Resin	**Viscosity (Pa·s)**	**Density (g/cm^3)**	**Refractive Index (n_o)**	**Cure Depth (µm)**
Resin1	0.53	1.01	1.477	1300.8 ± 37.8
Resin2	1.43	1.14	1.483	1356.0 ± 35.4

3. The Viscosity of Suspensions as a Function of Time

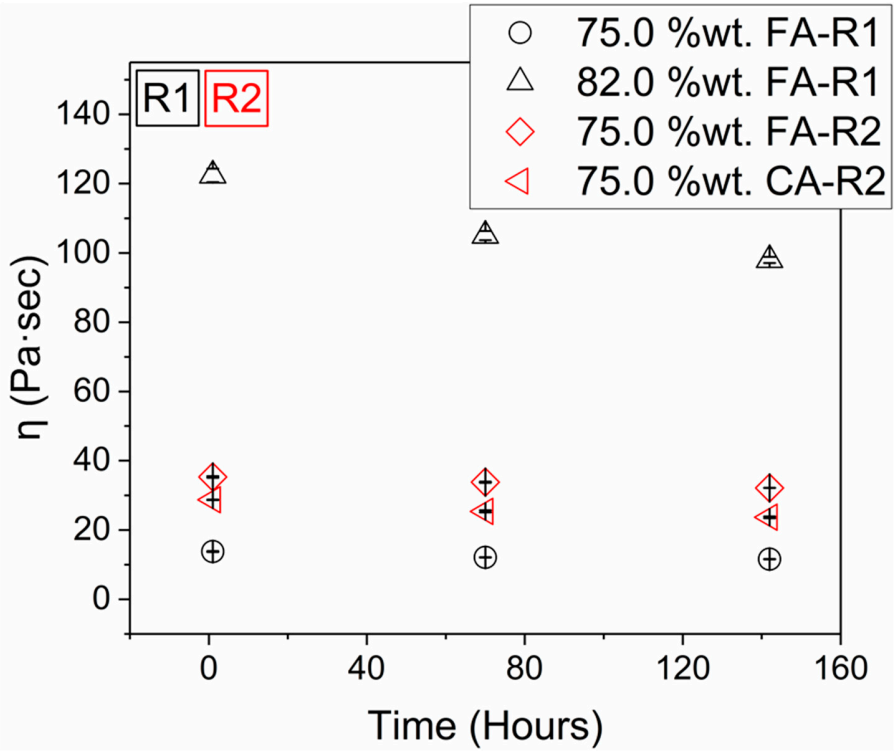

Figure S2. Viscosity of suspensions over time. The viscosity was measured at a shear rate of 1.0 sec^{-1} at 25.0 °C using a parallel plate with a diameter of 25.0 mm, and the gap between them was 1.0 mm. The test reflects three trials with a standard deviation error.

4. Printing Variables

Table S2. Energy doses and targeted cure depth that used for printing. The energy dose for printing was referred to as high energy dose when it is > 20.0 mJ/cm^2 and low energy dose when < 20.0 mJ/cm^2.

Solid Content (%wt.)	Resin	Powder	Layer Thickness (µm)	Energy Dose (mJ/cm^2)	Targeted Cure Depth/Layer Thickness Ratio
75.0	Resin1	AA07	20.0	14.7	7×
			50.0	14.7	3×
			50.0	88.9	7×
80.0			20.0	18.6	7×
82.0			20.0	15.5	7×
75.0	Resin2		20.0	11.8	7×
			50.0	11.5	3×
			50.0	69.8	7×
		AA3	20.0	6.2	7×
			50.0	6.2	3×
			50.0	24.4	7×

5. Debinding and Sintering Profiles

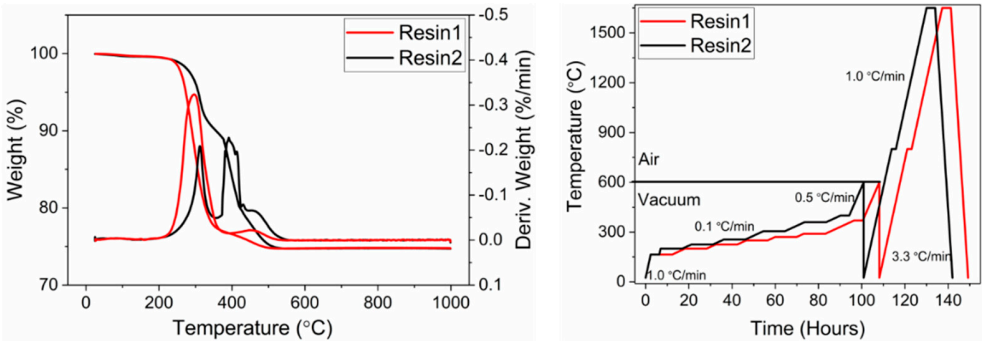

Figure S3. Thermal gravimetric analysis and thermal degradation and sintering profiles of Resin1 and Resin2. Prior debinding, the samples were submerged in warm deionized water for 24 hours, followed by drying for a minimum of 12 hours in air or a shorter duration using vacuum oven. However, this practice showed no impact on the samples.

6. Low Magnification FESEM Images of As-Printed Samples

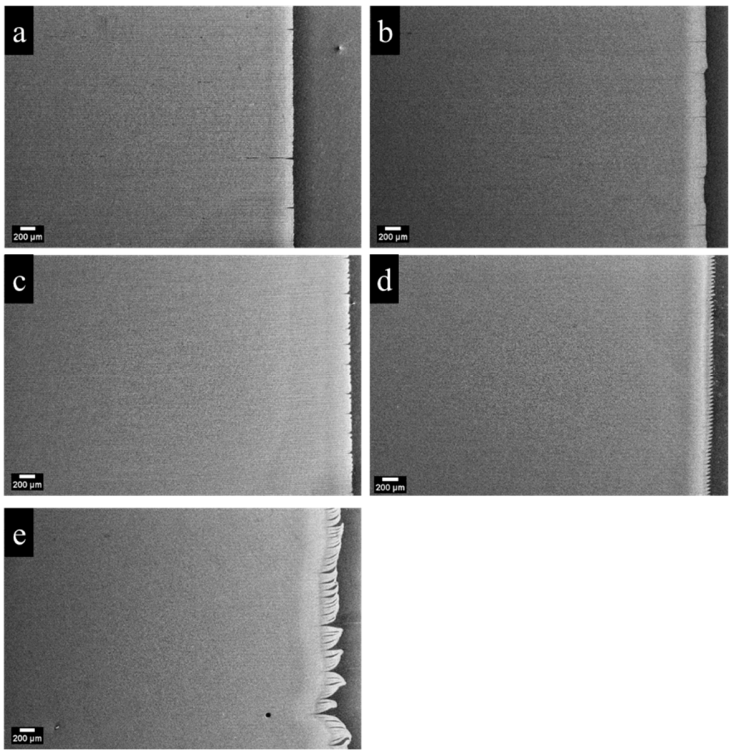

Figure S4. Scanning electron microscope images of as-printed samples. It is a low magnification to show the length of the cracks at the surface in few samples. Samples (Resin1 and AA07 powder) with solid content of (a) 75.0 %wt. and (b) 82.0 %wt., they were printed using 20.0 µm layer thickness and low energy dose. Samples (Resin2 and 75.0 %wt. AA07 powder) were printed using (c) 20.0 µm layer thickness and low energy dose, (d) 50.0 µm layer thickness and low energy dose, and (e) 50.0 µm layer thickness and high energy dose.

7. Interlayer Between the Base and First Layer

The strong scattering degree also showed a large interlayer portion between the base and first layer. Printing a single layer under these conditions on a base showed that the first interlayer had a thickness of 12.0 – 111.0 μm (Figure S5a). However, measuring the first interlayer in full prints revealed that its size was between none to about 179.0 μm (Figure S5b-d). These measurements were higher than what was seen in printing single layer experimentation due to the difference in microscope resolution. The interlayer portion was not observed between the rest of the layers in all the samples. This interlayer added additional difficulty to measure the dimensions in the building direction, but it was somewhat avoided during the measurements to obtain reliable dimensions. The results also showed a bulky portion on the side at the first few layers in a few samples (Figure S5b). This was believed to be caused by the additional curing of the coating outside the first few layers, which happened due to a strong scattering degree. This was reduced to none or a very small bulky portion when the scattering degree was lowered (Figure S5c and d).

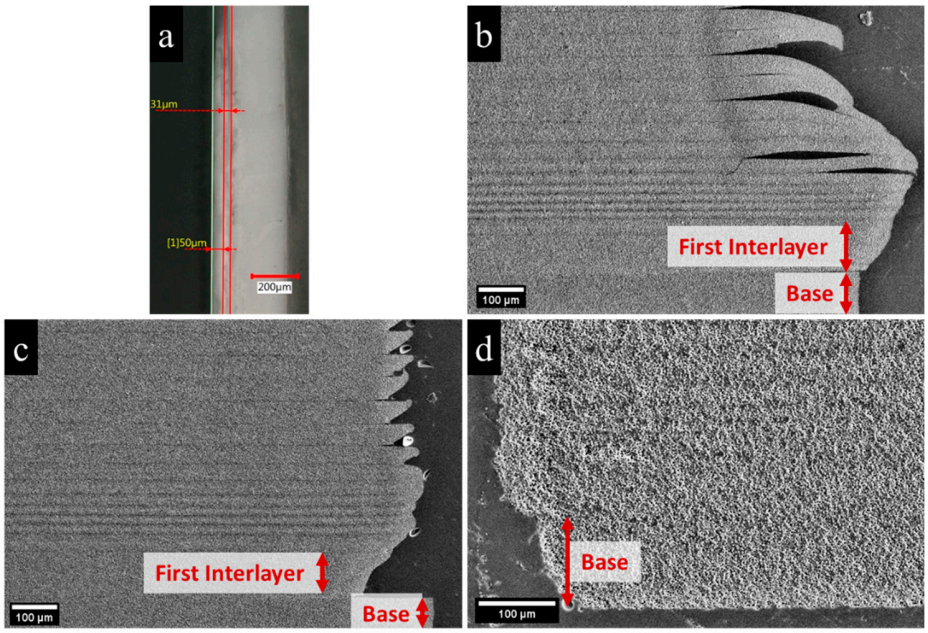

Figure S5. Optical and scanning electron microscope images of the first few layers and the first interlayer between the base and first layer of samples composed of Resin2 and 75.0 %wt. solid. They were printed using 50.0 µm layer thickness with different energy doses. (a) A single layer with a base only and (b – d) full prints. (a) and (b) as-printed samples (AA07 powder) that were printed using high energy dose. (c) as-printed sample (AA07 powder) that was printed using low energy dose. (d) as-debound sample (AA3 powder) that was printed using high energy dose.

8. Microstructure Images Post Debinding

The debinding profiles (Figure S3) worked well with samples printed using 20.0 µm layer thickness and low energy dose. They did not result in severe cracks affecting the dimensional measurements in a similar manner to the 50.0 µm layer thickness samples. The debinding did not result in any additional small cracks in most of the 20.0 µm layer thickness samples, but there were small internal cracks and growth in the surface openings in Resin1 samples only (Figure S6). We need to indicate that the scanning electron microscope imaging was conducted on limited samples; therefore, the number of internal cracks can not be verified. The samples with 50.0 µm layer thickness were excluded from further experimentation, and the post sintering dimensional

measurement was conducted only on samples composed of AA07 powder and printed using 20.0 µm layer thickness.

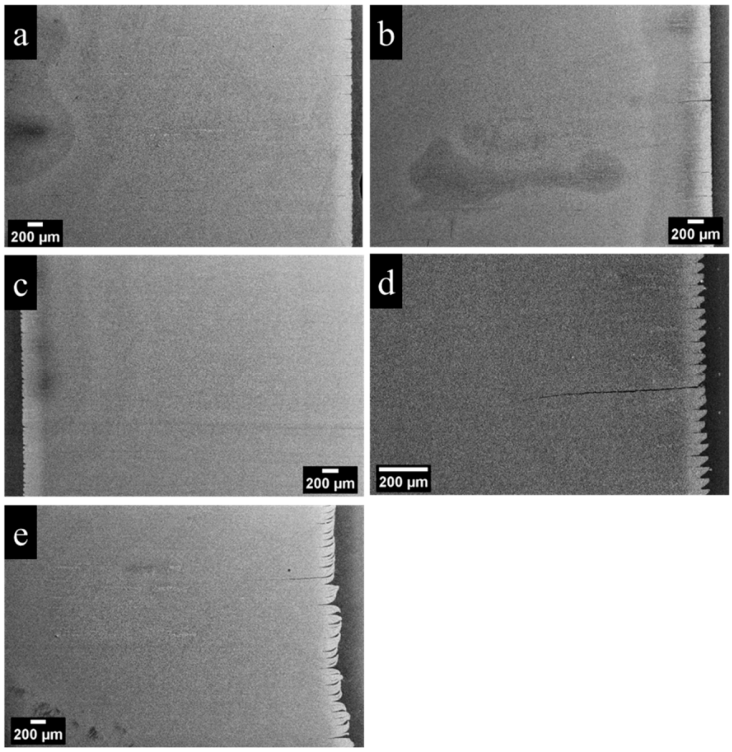

Figure S6. Scanning electron microscope images of as-debound samples. Samples (Resin1 and AA07 powder) with solid content of (a) 75.0 %wt. and (b) 82.0 %wt., they were printed using 20.0 µm layer thickness and low energy dose. Samples (Resin2 and 75.0 %wt. AA07 powder) were printed using (c) 20.0 µm layer thickness and low energy dose, (d) 50.0 µm layer thickness and low energy dose, and (e) 50.0 µm layer thickness and high energy dose.

9. Changes in the first layers using printers with thick and thin glass plates

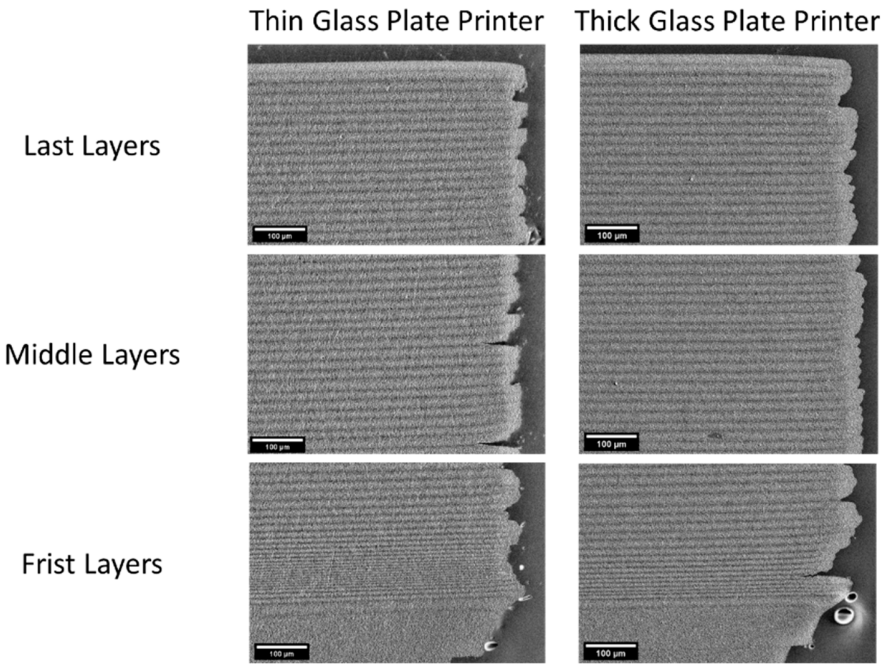

Figure S7. Scanning electron microscope images of as-printed samples using printer with thin glass plate vs thick glass plate. The 75.0 %wt. FA-R2 samples printed using 20 µm layer thickness.

Table S3. dimensional changes of samples using thin glass plate vs thick glass plate printers. The 75.0 %wt. FA-R2 samples printed using 20 µm layer thickness.

%	x	y	z
Thin glass plate printer	3.18 ± 0.14	3.19 ± 0.16	-7.98 ± 0.16
Thick glass plate printer	2.06 ± 0.34	2.20 ± 0.30	-3.85 ± 0.08

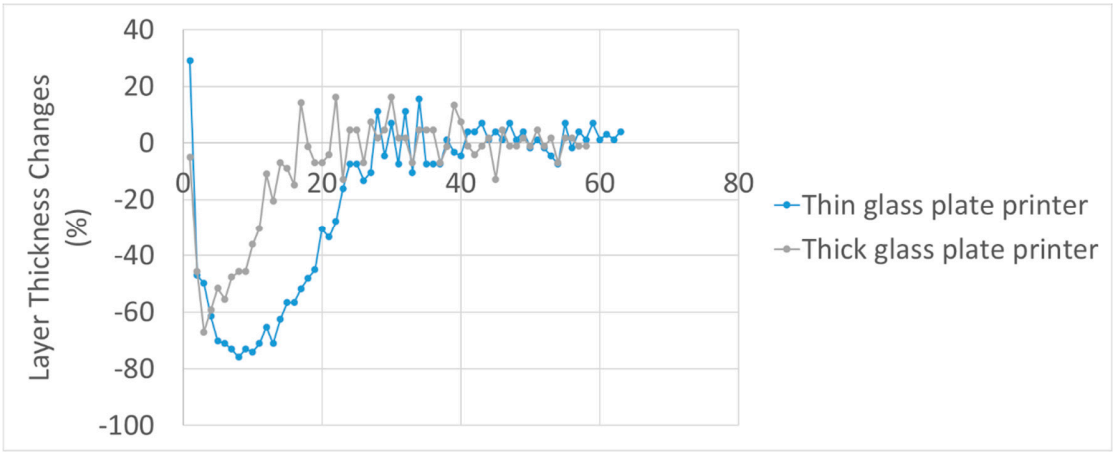

Figure S8 The changes in layer thickness across the prints of samples using thin glass plate vs thick glass plate printers. The 75.0 %wt. FA-R2 samples printed using 20 µm layer thickness.